Atmos. Chem. Phys. Discuss., 10, 26931–26959, 2010
www.atmos-chem-phys-discuss.net/10/26931/2010/
doi:10.5194/acpd-10-26931-2010

Atmospheric Chemistry and Physics Discussions

Aerosol nucleation spikes in the planetary boundary layer

J.-P. Chen[1], **T.-S. Tsai**[1], **and S.-C. Liu**[1,2]

[1]Department of Atmospheric Sciences, National Taiwan University, Taiwan
[2]Research Center of Environment Changes, Academia Sinica, Taiwan

Received: 27 August 2010 – Accepted: 14 September 2010 – Published: 9 November 2010

Correspondence to: J.-P. Chen (jpchen@as.ntu.edu.tw)

Published by Copernicus Publications on behalf of the European Geosciences Union.

Abstract

Photochemically driven nucleation bursts, which typically occur in a few hours after sunrise, often produce strong aerosol number concentration (ANC) fluctuations. The causes of such ANC spikes were investigated using a detailed aerosol model running in the parcel mode. Two potential mechanisms for the ANC spikes are proposed and simulated. The blocking of actinic flux by scattered clouds can significantly influence new particle production, but this does not cause strong fluctuations in the number of aerosols within sizes greater than the detection limit of our measurements. A more plausible mechanism is the turbulence eddy effect. Strong aerosol nucleation may occur in both updrafts and downdrafts, while the cloud formation at the boundary layer top strongly reduces the number of aerosols. As the number of aerosols is sensitive to turbulence eddy and cloud formation properties, a changing turbulence condition would result in large fluctuations in the evolution of ANC similar to that observed at the surface.

1 Introduction

Strong aerosol production in the planetary boundary layer (PBL) has been observed over various parts of the continents and oceans (cf., Dinger et al., 1970; Hegg et al., 1990; Covert et al., 1992; O'Dowd et al., 1998; Kulmala et al., 2004). How such productions occur deserves special attention as aerosols can influence human life in many aspects, such as air pollution, visibility, convective precipitation, as well as the climate impact through the modification of cloud structures (cf., Ozkaynak and Thurston, 1987; Quinby-Hunt et al., 1997; Khain et al., 2005; Levin and Cotton, 2007; Albrecht, 1989; Charlson et al., 1992; Ackerman et al., 1993). Besides direct emission or atmospheric transport, the nucleation process is considered an important source of aerosol particles in PBL. Aerosol nucleation in PBL often occurs during the daytime in the form of bursts that typically take only a few hours to complete. Sometimes the duration can be

ACPD
10, 26931–26959, 2010

less than one hour (Marti, 1990; Marti et al., 1997; Clarke et al., 1998; O'Dowd et al., 1998; Clement et al., 2001). Such an aerosol burst phenomena can be demonstrated with an event (Fig. 1) observed during the spring of 2003 at the Shimen sampling site located in Northern Taiwan. The measurement by an aerosol size spectrometer TSI SMPS-3934 (sampling frequency of about 7 min) showed a rapid increase in aerosol number concentration (ANC) after sunrise and reached a peak before noon. To rule out the possibility of aerosol increase due to long-range transport, one may further examine the fraction of freshly produced particles (here defined as those with a diameter of <30 nm). The nuclei mode particles do not stay long in the smallest size range because of either fast condensation or being collected by old particles. So, a fresh-to-total number ratio above approximately 0.4 (which may vary with the definition of fresh particles) is a good indication of a nucleation event. The one shown in Fig. 1 is apparently a nucleation burst as the "fresh" fraction increased simultaneously with the number production. Various modelling studies have shown that such nucleation bursts occur under clear or partly cloudy sky when photochemical production of sulfuric acid vapour is active (e.g., Harriton and Kreidenweis, 1998; Pirjola et al., 2000; Korhonen et al., 2004; Hellmuth, 2006a). However, the simulated aerosol number concentrations usually increase rather smoothly, whereas the observed ones often contain many spikes, as shown in Fig. 1. Such high-frequency spikes exist not only in the number concentration, but also in the fresh-particle fraction.

The Shimen site is located at the top of a small cliff 78 m in height and about 100 m distance from the open ocean that it faces. As the surrounding area is only sparsely populated, the only known source of local pollution is automobiles on a provincial, coastal highway underneath the cliff. For the event shown in Fig. 1, the prevailing northerly winds were blowing onto the shore, so the chances of them containing fresh anthropogenic emissions should be low. One cannot completely rule out the occasional passage of emission plumes from nearby ships or automobiles. Yet, such a phenomenon has also been observed in other relatively remote areas (e.g., O'Dowd et al., 1999; Coe et al., 2000; Guo et al., 2008), distant from human influence. Therefore,

ACPD
10, 26931–26959, 2010

looking into other possible mechanisms that may be responsible for the ANC spikes is worthwhile. Note that the time resolution in Fig. 1 is relatively coarse, and the spikes feature can be much finer as shown in some of these measurement studies.

Earlier postulations of the causes for small particle production include the shattering of salt formed by the rapid evaporation of cloud drops (e.g., Dessens, 1949; Twomey and McMaster, 1955; Radke and Hegg, 1972), but Mitra et al. (1992) disproved this mechanism with wind tunnel experiments. A more plausible cause for generating such nuclei-mode aerosols is homogeneous nucleation from the gas phase. Traditionally, homogeneous nucleation of atmospheric particles is thought to occur via the H_2O–H_2SO_4 binary interaction (Nair and Vohra, 1975; Yue and Hamill, 1979). Nucleation enhancement is possible with the presence of an additional gas such as ammonia (Coffman and Hegg, 1995; Yu, 2006), volatile organic compounds (O'Dowd et al., 1998), and aromatic acids (Zhang et al., 2004). Such processes are called ternary nucleation. Other nucleation mechanisms are also possible, but are irrelevant in this study.

According to the classical nucleation theory, the main conditions favourable for binary or ternary homogeneous nucleation are high water vapour saturation ratio S_w (relative humidity) and sulfuric acid vapour saturation ratio S_a (relative acidity), as well as low temperatures. Defined as the ambient vapour pressure divided by the saturation vapour pressure, the saturation ratio may be elevated by either an increase in vapour concentration or by lowering the temperature, thus, the saturation vapour pressure. The increase in water vapour concentration usually involves evaporation from the Earth's surface or airborne raindrops. The increase in sulfuric acid concentration, on the other hand, usually requires strong photochemical production which, in turn, demands high concentrations of precursor gas (e.g. SO_2) and high actinic flux to generate OH radicals for the reaction to occur. For the sulfuric acid to accumulate in the air, a low concentration of existing aerosols is also requires, which tends to consume the acid vapour needed for nucleation (Shaw, 1989; Petters et al., 2006).

A few physical conditions (i.e. the lowering of temperature) favourable to aerosol particle nucleation have also been investigated. The most common way to cause a fast

ACPD
10, 26931–26959, 2010

cooling is adiabatic expansion during ascending motion. Easter and Peters (1994) and Nilsson et al. (2001) suggested that turbulence in a well-mixed boundary layer may cause temperature fluctuations and induce new particle formation. Nilsson et al. (2000) also indicated that the upward motion of atmospheric waves could enhance aerosol nucleation. Another way of causing cooling is mixing. Bigg (1997) hypothesized that sudden mixing caused by the breaking of Kelvin-Helmholtz waves may induce strong aerosol nucleation. Similar mechanisms including turbulence mixing have also been investigated by Lesniewski and Friedlander (1995), Nilsson and Kulmala (1998), Khosrawi and Konopka (2003) and Wehner et al. (2010). Cooling due to long-wave radiation is usually too slow to cause strong nucleation.

A combination of some of the above factors is even more sufficient, if not necessary, for aerosol nucleation. Perry and Hobbs (1994) proposed that convective clouds bring up SO_2 (precursor to sulfuric acid) by cloud venting and removes a large portion of the existing aerosols by cloud and precipitation scavenging. High relative humidity and reflected sunlight near the clouds together form a favourable nurturing environment for new particles. However, the mechanisms mentioned above, acting individually or in combination, seem to be insufficient in explaining the occurrence of ANC spikes. A straightforward photochemical mechanism, as simulated by previously mentioned aerosol models, occurs in the diurnal time scale corresponding to the variation in solar radiation. Other effects that occur in a much shorter time scale are necessary to explain the spike phenomenon. One such candidate is the blocking of actinic flux by reoccurring scattered clouds, such as stratocumuli. This effect is one of the main themes of this study. Mixing induced cooling is not the likely mechanism for PBL spikes as it requires the involved air parcels to have distinctly different potential temperatures and the mixing occurs with strong fluctuations, which is apparently not the case under the synoptic conditions for the event in Fig. 1. On the other hand, cooling induced by turbulence does have a time scale similar to the observed ANC spikes and this phenomenon is very common in PBL. In addition, as will be demonstrated later, turbulence motion has an additional effect of providing a source for sulfuric acid vapour.

ACPD
10, 26931–26959, 2010

This study investigates the possible role of cloud shadowing and turbulence motion in ANC spike generation that shown in Fig. 1. As the phenomena, that we intend to examine, occur at rather fine spatial and temporal scales, they cannot be handled easily with typical Eularian models. The Largangian parcel model is quite suitable for our study as it allows finer details in aerosol microphysics and its dynamics can be prescribed to fit our purpose. In the following, we present several simulations from the aerosol parcel model and discuss possible mechanisms for ANC spikes.

2 Aerosol parcel model and simulation setup

The Lagrangian parcel model applied for this study was modified from the multi-component particle model of Chen and Lamb (1994, 1999), which allows simultaneous and independent changes in various physical and chemical properties of aerosol and cloud particles. For this study, two bin-components – water mass m_w and sulfate mass m_s – are used for the particle framework, with 45 bins each assigned for m_w and m_s. The lower limits of the largest bin for m_w and m_s are 2.3×10^{-10} mol and 5.6×10^{-11} mol (roughly equivalent to 10 µm radii), respectively. A bin-sizing factor of 2 is applied to successively smaller bin limits, except for the first and last bins having relaxed upper and lower boundaries, respectively, to cover extreme conditions. A method-of-moments type scheme is used to conserve mass and the number of particles, as well as reduce numerical diffusion, for their redistribution within the particle framework due to various growth mechanisms.

The growth mechanisms considered include binary nucleation and condensation growth from water and sulfuric acid vapours, as well as Brownian coagulation between particles. For the binary nucleation, we applied the classical theory for the water-sulfuric acid system with Zeldovich factor modification (cf., Doyle, 1961; Seinfeld and Pandis, 2006, 514–520) but ignored the hydrate formation effect. Condensation growth from both water vapour and sulfuric acid follows the Maxwellian two-stream theory with consideration of the curvature and solute effects on the particle surface vapour

ACPD
10, 26931–26959, 2010

pressures, as well as the surface gas-kinetic effect (cf., Pruppacher and Klett, 1997). Coagulation between particles is calculated using the Brownian collision kernel from Fuchs (1964) and a unity coagulation efficiency. Cloud formation may occur in some of the simulations. For this, the model does consider aerosol activation into cloud drops according to the Köhler theory. The condensation growth of cloud drops are treated the same as for the aerosol particles. Our model also considers the collision-coalescence between cloud drops, as well as interstitial (un-activated) aerosol collection by cloud drops. To focus on microphysical aerosol processes, a simple treatment is applied to the gas-phase production of sulfuric acid vapour. This production is assumed to come solely from SO_2 oxidation by OH, with a clear-sky reaction rate parameterized as a sinusoidal function of time to mimic the diurnal change in actinic flux and OH concentration according to an offline calculation from a photochemical model initialized with typical trace gas concentrations for the Shimen area.

The key parameters needed for the above calculations include the saturation vapour pressure of sulfuric acid from Jaecker-Voirol et al. (1990), saturation vapour pressure for water from Tabata (1973), solution water activity and sulfuric acid activity from Jaecker-Voirol and Mirable (1989), surface tension of sulfuric acid solution according to the experimental data of Morgan et al. (1916) fitted as a function of the concentration and temperature (and for the latter the Eötvös rule is applied), and the solution density data from the CRC Handbook for Physics and Chemistry. Note that large uncertainties exist in the calculation of nucleation rate from the classical theory, partly due to the ambiguity in these thermodynamic parameters which the nucleation rate is very sensitive to. Also note that, as pointed out by Korhonen et al. (1999), while some studies showed that predictions of binary nucleation from H_2SO_4 and H_2O are consistent with the measured new particle formation, others indicated that such binary nucleation may be too weak to explain the observed particle production, and the latter seems to be particularly true for the marine boundary layer or continental sites (conditions similar to that for Fig. 1). Yet, our calculation seems to give reasonable results. One possible reason for us to obtain sufficiently high nucleation rates is that we considered this size

ACPD
10, 26931–26959, 2010

effect on surface tension. Tolman (1949) pointed out that surface tension may be significantly less than its bulk value when the particle is small, especially for the nucleation embryos and nuclei-mode particles. This effect has a strong influence on the nucleation and condensation processes, but is not considered in most aerosol models. In our model this effect has been included according to the treatment of Chen et al. (2008). Because of several limiting factors, such as the depletion of vapours by the growth of newly formed particles or the coagulation to existing large particles, the overall number of new particle production actually does not vary too strongly with the nucleation rate. Therefore, inaccuracy in the nucleation rate does not lead to an equally large error in the total production of new aerosols.

Several simulations are designed to examine the two effects relevant to the ANC spikes phenomenon. The cloud-shadow effect is considered by imposing a reduction of the transmitted actinic flux (thus, the production of sulfuric acid vapour) for the scattered stratocumulus clouds (Sc) situation. The turbulence cooling effect is considered by giving the air parcel a large-eddy type of motion. Both the stratocumuli and turbulence eddies are quite common to the area of study during spring when the PBL is dominated by the continental cold-air outflow. The stratocumuli formation near the top of PBL is associated with the mechanically forced turbulence eddy in PBL, where clouds form in the ascending region and dissipate during descends. Air parcels in such a turbulent environment tend to have wave-like motions as demonstrated by the trajectory analysis of Feingold et al. (1998). Therefore, the turbulence air parcel is assumed to move up and down adiabatically following a sinusoidal trajectory. According to the results of Feingold et al. (1998), we selected a cycling period of 30 min and semi-amplitude of 500 m for our main simulations, but other values were also tested. The same sinusoidal function was also used to calculate the attenuation of actinic flux below the stratocumuli, such that the actinic flux oscillates from a specified minimum value (at the centre of cloud shadow) to a clear-sky value. Also simulated for comparison is the influence of stratus clouds (St) which are assumed to distribute uniformly in space and time.

ACPD
10, 26931–26959, 2010

The simulations also need to consider the presence of existing aerosol particles as they may consume sulfuric acid vapour and hinder the nucleation process. The initial size distribution is assumed to be a bi-modal log-normal function (cf., Whitby, 1978), parameterized according to the mean size distribution measured at Shimen during March and April of 2003. Its total number concentration of 2690 cm^{-3} represents a relatively clean rural condition. For comparison purposes, we also applied an average aerosol size distribution measured in the city of Taipei (located 30 km south of Shimen), with a total number concentration of 15 080 cm^{-3} representing urban conditions.

For the simulation of either the Sc or St cloud-shadow effects, the air temperature and relative humidity of the air parcel were fixed at 20 °C and 75%, respectively, which are typical ambient conditions at sunrise for the situation studied here. Although in reality, the temperature and relative humidity of the PBL air do vary with time due to solar heating and other meteorological factors, they are fixed so that a direct comparison can be made with the turbulence simulations for which the air parcel is assumed to proceed adiabatically. The effect of varying ambient conditions will be discussed.

3 Simulation results

Let us first examine a simpler cloud-shadow effect case – the uniform St clouds – for the conditions at Shimen. As shown in Fig. 2a, the aerosol number concentration increases drastically after sunrise due to sulfate photochemical production. Under clear skies, the number of aerosols may increase by two orders of magnitude. When the actinic flux is attenuated by uniform clouds (represented by a transmission ratio Q), the burst of aerosols is reduced in magnitude as well as delayed in time. Note that, unlike Fig. 2a which includes aerosol particles of all sizes (denoted as D-all), the measurements with the TSI SMPS-3934 for this study covered only particles from 10 to 500 nm in diameter (with 102 intervals). To give a fair comparison with observations, we show in Fig. 2b only particles with diameters larger than 10 nm (denoted as D>10). Here, the nucleation burst is still evident and the maximum number concentration is now of

ACPD
10, 26931–26959, 2010

a similar magnitude as the observation that is shown in Fig. 1. The large decrease in particle number for D>10 indicates that either the fresh particles growth by condensation is slow, or the fresh particles collection by the larger old particles is strong. Comparing Fig. 2b with Fig. 1, one can see that the simulated nucleation burst started 1–2 h earlier than observed, except when the photochemical production is very weak (Q~0.2), which is not likely in the real case. Yet, when the observed temperature and relative humidity variation (instead of at fixed values) were applied in the simulations, the timing of the nucleation burst is delayed mainly because of lowered humidity and becomes more comparable with Fig. 1.

Similar to other aerosol model results, the nucleation burst shown in Fig. 2 lacks the spikes feature shown in Fig. 1. Additional mechanisms must exist to produce such spikes. Next, we examine whether intermittent cloud shadows due to re-occurring stratocumulus may be one of the causes. Figure 3 shows the simulations with imposed sinusoidal attenuation of the actinic flux due to stratocumulus, with the transmission ratio varying periodically from unity to a minimum value denoted by Q. Note that the curves for Q=1 represent a total transmission, thus, they are exactly the same as those for the clear sky condition in Fig. 2. From Fig. 3a one can see that new particles are generated during cloud breaks when there is sufficient sulfuric acid vapour production by photochemistry. Under cloud shadows, the particle number actually decreased rapidly, because of reduced photochemistry and a strong coagulation of the newly formed particles with the existing ones. Such a sharp fluctuation repeats itself for each cloud cycle when there is sun light. The particle reduction during the cloud-shadow period actually helps the nucleation later because the existing aerosols become fewer, thus, less capable of consuming sulfuric acid vapour by condensation. This effect can be seen clearly from the higher maximum number concentrations during cloud breaks than that for the all clear sky condition (Q=1). The fluctuation of particle number for D>10 becomes much less significant although still visible (Fig. 3b).

The cloud-shadow effect seems to be able to cause fluctuations in particle nucleation. But the amplitudes of fluctuation for D>10 are much less striking than the ob-

ACPD
10, 26931–26959, 2010

served spikes shown in Fig. 1. Apparently a different mechanism is required to explain the observation. As will be shown, the mechanism of turbulence-induced nucleation is quite capable of causing stronger fluctuations in nucleation.

To simulate the effect of large eddy turbulence, the air parcel is assumed to rise and sink adiabatically following a sinusoidal vertical path. In the rising part of the eddy, the expanding air cools down rapidly and the lowering temperature causes an increase in both S_w and S_a, which leads to enhanced nucleation. Clouds often form at the top of the large eddies in PBL. For the results shown below, the S_w of air parcel varies from 64% at the surface to about 80% at mid-level and reaches over 100% near the top where clouds are formed. Other conditions are the same as those for previous simulations. Also imposed are reductions in actinic flux similar to those specified for the St simulations in Fig. 2. In Fig. 4a, one can see the large eddy motions caused a pulsating production of aerosols similar to that shown in Fig. 3a, but with significantly stronger amplitudes. For $D>10$ (Fig. 4b), the fluctuation is still obvious and much more significant than that in Fig. 3b, except for $Q<0.2$ for which the variation becomes insignificant. When $Q=1$, both the peak number concentration and the spike features are quite similar to those shown in Fig. 1.

However, the cause of the pulsating particle bursts is not just a simple effect of cooling-enhanced nucleation. In fact, one may have noticed some irregularities in the evolution of particle number concentration in Fig. 4 as compared with Fig. 3. The details can be revealed by zooming up a couple of the cycles. As the behaviour of each cycle is similar, we will focus on the two cycles occurring between 11h00 and noon. In Fig. 5a, one can find two peaks in the number concentration in each cycle in contrast to the single peak in Fig. 3. The situation for $D>10$ is even more complicated. To understand this result, we need to examine parameters most critical to the binary nucleation – the relative humidity S_w and relative acidity S_a of the air parcel.

The ups and downs of S_w shown in Fig. 6a basically reflect the imposed periodical variation in vertical motion. So, S_w increases in the updraft due to expansion cooling and decreases in the downdraft due to compression warming. The expansion cooling

ACPD
10, 26931–26959, 2010

should in principle also cause an increase in S_a provided that the sulfuric acid vapour mixing ratio is kept constant. Yet, the simulation shows that the variation in S_a is out of phase with S_w, indicating an additional source or sink for sulfuric acid vapour. The formation of clouds, as indicated by the development of supersaturation (S_w>1), at the tops of the circulation play an important role here. In fact, S_a is the lowest when the air parcel is inside the cloud (the reason for which will be explained later). Then, it increases rapidly in the downdraft after the clouds have dissipated. Since the photochemical production of sulfuric acid vapour varies only slowly during the hour (dashed curve in Fig. 6b), the increase in S_a in the downdraft must be due to slower sulfuric acid vapour condensation (dotted curve in Fig. 6b). This retarded condensation is mainly a consequence of the drastic reduction in existing particles in the clouds. This reduction has two main causes. First, Brownian collection is greatly enhanced due to the large size of the cloud drops. Second, the growth of cloud drops by water vapour condensation considerably reduces the Henry's law surface pressure of sulfuric acid vapour, and this leads to a thermodynamic imbalance between the cloud drops and interstitial particles whose surface vapour pressures are elevated due to the large curvature effect. Therefore, the cloud drops can uptake sulfuric acid in the expense of evaporating interstitial aerosols, and some of the smaller ones may evaporate completely if they are not already collected by the cloud drops. So, in the downdraft, after the clouds have dissipated, the number of aerosol particles for the sulfuric acid vapour to condense on is very low. This leads to a buildup of S_a (Fig. 6a) which is favourable to nucleation (Fig. 6b). Hence, the particle number shoots up at about 11h11 (and 11h41) as shown in Fig. 5. A second mechanism which leads to a slower sulfuric acid vapour condensation in the downdraft is the drying of air parcels (i.e. lowing S_w) as a result of adiabatic warming. The drying effect causes the particles to lose water and their dissolved sulfuric acid becomes more concentrated. The reduction in size and the elevation of solute concentration both lead to a slower sulfuric acid vapour condensation. In spite of the overall positive rate of condensation shown in Fig. 6b, the smallest ones actually are evaporating, thus, becoming a source (besides photochemical production)

ACPD
10, 26931–26959, 2010

of sulfuric acid vapour to the large particles. The smallest aerosol particles may evaporate completely as a result. In the later part of the downdraft, the nucleation becomes very weak due to the lowering of S_w, even though S_a at the time is still increasing. So, at about 11h23, the production by nucleation is not enough to compensate for the loss due to collision or complete evaporation and the particle number reaches its secondary minimum.

A second nucleation spike (of the same cycle) occurs in the updraft. It starts at about 11:24 when S_w begins to increase due to adiabatic cooling and while S_a is still building up (because the photochemical production of sulfuric acid vapour is still stronger than the loss by condensation). This updraft-induced spike is stronger than that in the downdraft in both magnitude and duration. It ends when the formation of new particles is so overwhelming that the sulfuric acid vapour condensation on the particles significantly exceeds the photochemical production. In addition, the swelling (and dilution) of existing particles due to increasing relative humidity also enhances condensation. The complete termination of nucleation (at around 11h37) happens when the air parcel reaches the condensation level, as the growing cloud drops quickly, absorbing sulfuric acid vapour and causing S_a to decrease to its lowest level.

The similarity between the Q=1 result in Fig. 4b and the observed result in Fig. 1 may give us a false impression that the answer has been found. However, there is a problem comparing Fig. 4b directly with Fig. 1, because the former was calculated following the undulating air parcel and, thus, cannot represent the situation at the surface. If only the surface values were plotted (i.e., connecting the lowest point of each cycle), one would see only a simple nucleation burst without all the spikes (similar to the Q=1 curve in Fig. 3b). But this discrepancy does not necessarily invalidate the turbulence-induced nucleation mechanism. For the results in Fig. 4, the physical parameters (e.g., frequency or amplitude) of the turbulence eddies were fixed, yet in reality they vary significantly with time and space. We will next demonstrate that such variations may be enough to cause the spikes in particle number concentration at the surface.

ACPD
10, 26931–26959, 2010

Figure 7 shows the evolution of $D>10$ particles for a few additional simulations of different turbulence eddies. Two earlier results are also included for comparison: (1) the thick-solid curve labelled "clear" is the clear-sky, no turbulence case, and is the same as the $Q=1$ curve in Fig. 3b; (2) the green curve labelled "0.5 h" (oscillation period of 0.5 h) is the reference case of turbulence eddy, and is the same as the $Q=1$ curve in Fig. 4b. Let us first look at two curves which contain some fluctuations but have baselines following close to the "clear" curve. These two cases applied the same conditions as the "0.5 h" case except that the mid-level relative humidity is lowered by 5% for the "RH75%" curve, whereas for the "H250" curve, the oscillation amplitude is reduced by one half. The reason for these two curves to behave so differently from their reference case is the absence of cloud formation due to either not enough moisture (RH75) or not enough vertical lift (H250). Earlier we have shown that clouds can effectively remove the existing particles. Without cloud formation, the near-surface concentration of $D>10$ particles stays not far from that of the clear-sky no-turbulence case. The next two simulations will demonstrate how sensitive the aerosol concentration is to the cloud properties.

The curves labelled "1 h" and "0.25 h" differ from the reference case in their doubled and halved oscillation period, respectively. As the amplitude of vertical movement remains unchanged, clouds are formed when the air parcel reaches the top, just like in the reference case. The three cases with cloud formations (e.g., the curves labelled "1 h", "0.5 h" and "0.25 h") not only behave differently from those without cloud formation but also exhibit large discrepancies among themselves. When clouds are present, the fluctuation in particle number is much stronger and the minimum particle number (representing the situation near the surface) is significantly lower, reflecting strong in-cloud processing of existing aerosols as discussed earlier. Such an effect is stronger for shorter oscillation periods for two reasons. Firstly, the time for nucleation to proceed in each cycle is shorter, so the accumulated particle number production is reduced. Secondly, this time factor also limits the growth of the newly produced particles to $D>10$ sizes. Therefore, the simulation with the shortest oscillation period (0.25 h) produced

ACPD
10, 26931–26959, 2010

the lowest particle number concentration and the weakest fluctuations.

As shown by Feingold et al. (1998) and others, the eddy-like movement of air parcels in the PBL often has large variations in amplitude and frequency. So, one can imagine that altering the paths of eddy motions would cause the surface particle number to fluctuate. Judging from the large differences shown in Fig. 7, the magnitude of the fluctuations from this mechanism should be enough to explain the ANC spikes in Fig. 1.

In either updrafts or downdrafts, the nucleation spikes generally are associated with a low amount of existing aerosol particles at a prior time. This implies that when the amount of existing aerosols is high, such as in an urban environment, nucleation might be prohibited even when there is a strong photochemical production of sulfuric acid (or other condensable vapours that may be involved in the nucleation process). To examine this prospect, we performed another set of simulations similar to those shown in Figs. 2–4, but the initial aerosol size distribution was switched to the urban (Taipei) type. Among all simulations, none produced a noticeable nucleation burst, not to mention spikes, in D>10 particles. Only the turbulence eddy case showed significant fluctuations in D-all particles (figures not shown). This result also implies that cloud processing becomes quite weak under polluted situations, as the cloud drops become much smaller although more numerous. So, a large amount of existing particles tends to suppress nucleation, as well as prohibits the nucleated particles to grow to the D>10 sizes.

4 Discussion and conclusion

This study applied a detailed aerosol model running in the parcel mode to investigate possible causes to the large fluctuations (spikes) in aerosol number concentration (ANC) in the planetary boundary layer (PBL) observed during a nucleation burst event. Two mechanisms for such ANC spikes were investigated: (1) cloud-shadow effect, and (2) turbulence eddy effect. These re-occurring effects have time scales of a few tens of minutes, roughly the same as that of the observed ANC spikes.

ACPD
10, 26931–26959, 2010

The cloud-shadow effect reduces the actinic flux that reaches the PBL, thus, reducing photochemical production of sulfuric acid vapour which is essential for binary nucleation occurrence. Simulations of this kind do produce large fluctuations in the evolution of total particle concentration. However, for particles with sizes above the instrument detection limit (larger than 10 nm diameter, denoted as $D>10$), the fluctuations are somewhat less obvious than observed. It is possible that the variation in actinic flux assumed in this study is not sharp enough to cause enough fluctuation in particle nucleation.

Mechanically forced large eddy motions in the PBL can cause much stronger fluctuations in $D>10$ particle number concentration, with magnitudes similar to those observed. The nucleation is enhanced mainly in the updraft, where cooling due to adiabatic expansion results in a sharp increase in the water saturation ratio. This updraft-mode nucleation benefits from the reduction in particles during the downdraft stage. Such updraft-mode nucleation has been investigated by Easter and Peters (1994) who concluded that nucleation can be enhanced at higher altitudes in PBL, and this view is shared by Clarke et al. (1998). However, our results in Fig. 6 show that the fastest increase in aerosol number occurred at lower altitudes before arriving at the mid-level PBL.

Another mode of nucleation may occur in the downdraft, particularly when there is cloud formation at PBL top. In the downdraft, adiabatic warming may cause the relative humidity and relative acidity to decrease, which is unfavourable for nucleation. But the drying effect also causes the solution in aerosol to become more concentrated and this prohibits sulfuric acid vapour condensation on the existing particles. Such an effect actually causes the relative acidity to increase in the downdraft, thus, favoring the nucleation of aerosols. The presence of clouds further enhances the downdraft-mode nucleation because of the collection of interstitial aerosol particles by cloud droplets. Once the cloud dissipated during the descending stage, the amount of existing particles has been significantly reduced so that their ability to consume sulfuric acid vapour is minimized, allowing the relative acidity to accumulate. Because of the higher altitude

ACPD
10, 26931–26959, 2010

that it occurs, this downdraft-mode nucleation may be relevant to the particle nucleation phenomenon observed in the vicinity of marine boundary layer clouds (e.g., Dinger et al., 1970; Hegg et al., 1990; Perry and Hobbs, 1994; Frick and Hoppel, 1993). Furthermore, Clarke et al. (1999) showed that the particle production occurred near the edges of evaporating clouds in marine PBL. They suggested that classical binary nucleation theory may be able to explain this phenomenon when high humidity and low existing particle concentration are applied. The downdraft-mode nucleation, simulated in this study, seems to fit these conditions quite well.

However, because the Lagrangian-type simulations cannot represent observations taken at a fixed location, the turbulence eddy effect shown above cannot be taken straightforwardly to explain the ANC spikes occurring at the surface. In fact, for the simulations in Figs. 5 and 6 that applied a fixed eddy size, particles number concentration at any given height does not exhibit fluctuations. Yet, the results in Fig. 7 suggested that the ANC spikes at the surface may occur if the properties (e.g., amplitude and frequency) of the turbulence eddy change with time. This is indeed the case as the vertical movement of turbulence eddies is known to evolve significantly with time (e.g. Feingold et al., 1998; Gibert et al., 2010). Cloud formation, in particular, can cause a large decrease in particle number. This means that the peaks of the spikes are caused by nucleation in air parcels that did not go through cloud processes, and the dips are from those that went through recent cloud formation. From the analyses above, we conclude that the turbulence eddy and cloud processing mechanism is a likely cause of the surface ANC spikes.

Acknowledgement. The study was supported by the Academia Sinica through the thematic project "Particulate Matter and its Environmental Impacts" as well as by projects NSC 98-2111-M-002-001 and NSC 99-2111-M-002-009-MY3.

ACPD
10, 26931–26959, 2010

References

Ackerman, A. S., Toon, O. B., and Hobbs, P. V.: Dissipation of marine stratiform clouds and collapse of the marine boundary layer due to the depletion of cloud condensation nuclei by clouds, Science, 262, 226–229, 1993.

Albrecht, B. A.: Aerosols, cloud microphysics, and fractional cloudiness, Science, 245, 1227–1230, 1989.

Bigg, E. K.: A mechanism for the formation of new particles in the atmosphere, Atmos. Res., 43, 129–137, 1997.

Charlson, R. J., Schwartz, S. E., Hales, J. M., Cess, R. D., Coakley Jr., J. A., Hansen, J. E., and Hofmann, D. J.: Climate forcing by anthropogenic aerosols, Science, 255, 423–430, 1992.

Chen, J.-P. and Lamb, D.: Simulation of cloud microphysical and chemical processes using a multicomponent framework. Part I: description of the microphysical model, J. Atmos. Sci., 51, 2613–2630, 1994.

Chen, J.-P. and Lamb, D.: Simulation of cloud microphysical and chemical processes using a multicomponent framework. Part II: microphysical evolution of a wintertime orographic cloud, J. Atmos. Sci., 56, 2293–2312, 1999.

Chen, J.-P., Hazra, A., and Levin, Z.: Parameterizing ice nucleation rates using contact angle and activation energy derived from laboratory data, Atmos. Chem. Phys., 8, 7431–7449, doi:10.5194/acp-8-7431-2008, 2008.

Clarke, A. D., Davis, D., Kapustin, V. N., Eisele, F., Chen, G., Paluch, I., Lenschow, D., Bandy, A. R., Thornton, D., Moore, K., Mauldin, L., Tanner, D., Litchy, M., Carroll, M. A., Collins, J., and Albercook, G.: Particle nucleation in the tropical boundary layer and its coupling to marine sulfur sources, Science, 282, 89–92, 1998.

Clarke, A. D., Kapustin, V. N., Eisele, F. L., Weber, R. J., and McMurry, P. H.: Particle production near marine clouds: sulfuric acid and predictions from classical binary nucleation, Geophys. Res. Lett., 26(16), 2425–2428, 1999.

Clement, C. F., Pirjola, L., dal Maso, M., Mäkelä, J., and Kulmala, M.: Analysis of particle formation bursts observed in Finland, J. Aerosol Sci., 32, 217–236, 2001.

Coe, H., Williams, P. I., McFiggans, G., Gallagher, M. W., Beswick, K. M., Bower, K. N., and Choularton, T. W.: Behavior of ultrafine particles in continental and marine air masses at a rural site in the United Kingdom, J. Geophys. Res., 105(D22), 26891–26905, 2000.

Coffman, D. J. and Hegg, D. A.: A preliminary study of the effect of ammonia on particle nucle-

ACPD
10, 26931–26959, 2010

ation in the marine boundary layer, J. Geophys. Res., 100(D4), 7147–7160, 1995.
Covert, D. S., Kapustin, V. N., Quinn, P. K., and Bates, T. S.: New particle formation in the marine boundary layer, J. Geophy. Res. D, 97, 20581–20589, 1992.
Dessens, H.: The use of spiders' threads in the study of condensation nuclei, Q. J. Roy. Meteor. Soc., 75, 23–23, 1949.
Dinger, J. E., Howell, H. B., and Wojciechowski, T. A.: On the sources and composition of cloud condensation nuclei in the subsidence air mass over the North Atlantic, J. Atmos. Sci., 27, 791–797, 1970.
Doyle, G. J.: Self nucleation in the sulfuric acid water system, J. Chem. Phys., 35, 795–799, 1961.
Easter, R. C. and Peters, L. K.: Binary homogeneous nucleation: temperature and humidity fluctuations, nonlinearity, and aspects of new particle production in the atmosphere, J. Appl. Meteorol., 33, 775–784, 1995.
Feingold, G. S., Kreidenweis, M., and Zhang, Y.: Stratocumulus processing of gases and cloud condensation nuclei: part I: trajectory ensemble model, J. Geophys. Res., 103, 19527–19542, 1998.
Fuchs, N.: The Mechanics of Aerosols, Pergamon Press, New York, 408 pp., 1964.
Frick, G. M. and Hoppel, W. A.: Airship measurements of aerosol size distribution, cloud droplet spectra, and trace gas concentrations in the marine boundary layer, B. Am. Meteorol. Soc., 74, 2195–2202, 1993.
Gibert, F., Koch, G. J., Beyon, J. Y., et al.: Can CO_2 turbulent flux be measured by lidar? A preliminary study, J. Atmos. Oceanic Tech., doi:10.1175/2010JTECHA1446.1, 2010.
Guo, H., Liu, Y., Daum, P. H., Senum, G. I., and Tao, W.-K.: Characteristics of vertical velocity in marine stratocumulus: comparison of large eddy simulations with observations, Environ. Res. Lett., 3, 045020, doi:10.1088/1748-9326/3/4/045020, 2008.
Hegg, D. A., Radke, L. F., and Hobbs, P. V.: Particle production associated with marine clouds, J. Geophys. Res., 95, 917–926, 1990.
Hellmuth, O.: Columnar modelling of nucleation burst evolution in the convective boundary layer – first results from a feasibility study Part I: Modelling approach, Atmos. Chem. Phys., 6, 4175–4214, doi:10.5194/acp-6-4175-2006, 2006a.
Hellmuth, O.: Columnar modelling of nucleation burst evolution in the convective boundary layer – first results from a feasibility study Part III: Preliminary results on physicochemical model performance using two "clean air mass" reference scenarios, Atmos. Chem. Phys., 6,

ACPD
10, 26931–26959, 2010

4231–4251, doi:10.5194/acp-6-4231-2006, 2006b.
Jaecker-Voirol, A. and Mirabel, P.: Homogeneous nucleation in the sulfuric acid-water system, Atmos. Environ., 23, 2053–2057, 1989.
Jaecker-Voirol, A., Ponche, J. L., and Mirabel, P.: Vapor pressures in the ternary system water-nitric acid-sulfuric acid at low temperatures, J. Geophys. Res., 95(D8), 11857–11863, 1990.
Khain, A., Rosenfeld, D., and Pokrovsky, A.: Aerosol impact on the dynamics and microphysics of deep convective clouds, Q. J. Roy. Meteor. Soc., 131, 1–25, 2005.
Khosrawi, F. and Konopka, P.: Enhanced particle formation and growth due to mixing processes in the tropopause region, Atmos. Environ., 37, 903–910, 2003.
Korhonen, P., Kulmala, M., Laaksonen, A., Viisanen, Y., McGraw, R., and Seinfels, J. H.: Ternary nucleation of H_2SO_4, NH_3, and H_2O_2 in the atmosphere, 104(D21), 26349–26353, 1999.
Korhonen, H., Lehtinen, K. E. J., and Kulmala, M.: Multicomponent aerosol dynamics model UHMA: model development and validation, Atmos. Chem. Phys., 4, 757–771, doi:10.5194/acp-4-757-2004, 2004.
Kulmala, M., Vehkamäki, H., Petäjä, T., Dal Maso, M., Lauri, A., Kerminen, V.-M., Birmili, W., and McMurry, P. H.: Formation and growth rates of ultrafine atmospheric particles: a review of observations, J. Aerosol Sci., 35, 143–176, 2004.
Lesniewski, T. and Friedlander, S. K.: The effect of turbulence on rates of particle formation by homogeneous nucleation, Aerosol Sci. Tech., 23, 174–182, 1995.
Levin, Z. and Cotton, W.: Aerosol pollution impact on precipitation: a scientific review. Report from the WMO/IUGG International Aerosol Precipitation Science Assessment Group, World Meteorological Organization, Geneva, Switzerland, 2007.
Marti, J.: Diurnal variation in the undisturbed continental aerosol: results from a measurement program in Arizona, Atmos. Res., 25, 351–362, 1990.
Marti, J. J., Weber, R. J., McMurry, P. H., Eisele, F., Tanner, D., and Jefferson, A.: New particle formation at a remote continental site: assessing the contributions of SO_2 and organic precursors, J. Geophys. Res., 102(D5), 6331–6339, 1997.
Mitra, S. K., Brinkmann, J., and Pruppacher, H. R.: A wind tunnel study on the drop-to-particle conversion, J. Aerosol Sci., 23, 245–256, 1992.
Morgan, J., Livingston, R., and Davis, C. E.: The properties of mixed liquids. I. Sulfuric acid-water mixtures, J. Am. Chem. Soc., 38555–38568, 1916.
Nair, P. V. N. and Vohra, K. G.: Growth if aqueous sulfuric acid droplets as a function of relative

ACPD
10, 26931–26959, 2010

humidity, J. Aerosol Sci., 6, 265–271, 1975.
Nilsson, E. D. and Kulmala, M.: The potential for atmospheric mixing processes to enhance the binary nucleation rate, J. Geophys. Res, 103(D1), 1381–1389, 1998.
Nilsson, E. D., Pirjola, L., and Kulmala, M.: The effect of atmospheric waves on aerosol nucleation and size distribution, J. Geophys. Res., 105(D15), 19917–19926, 2000.
Nilsson, E. D., Rannik, Ü., Kulmala, M., Buzorius, G., and O'Dowd, C. D.: Effects of continental boundary layer evolution, convection, turbulence and entrainment, on aerosol formation, Tellus, 53B, 441–461, 2001.
O'Dowd, C. D., Geever, M., Hill, M. K., Smith, M. H., and Jennings, S. G.: New particle formation: nucleation rates and spatial scales in the clean marine coastal environment, Geophys. Res. Lett., 25(10), 1661–1664, 1998.
O'Dowd, C. D., McFiggans, G., Creasey, D. J., et al.: On the photochemical production of new particles in the coastal boundary layer, Geophys. Res. Lett., 26, 1707–1710, 1999.
Ozkaynak, H. and Thurston, G. D.: Associations between 1980 US mortality rates and alternative measures of airborne particle concentration, Risk Anal., 7, 449–461, 1987.
Perry, K. D. and Hobbs, P. V.: Further evidence for particle nucleation in clear air adjacent to marine cumulus clouds, J. Geophys. Res., 99, 22803–22818, 1994.
Petters, M. D., Snider, J. R., Stevens, B., Vali, G., Faloona, I., and Russell, L. M.: Accumulation mode aerosol, pockets of open cells, and particle nucleation in the remote subtropical Pacific marine boundary layer, J. Geophys. Res., 111, D02206, doi:10.1029/2004JD005694, 2006.
Pirjola, L., O'Dowd, C. D., Brooks, I. M., and Kulmala, M.: Can new particle formation occur in the clean marine boundary layer?, J. Geophys. Res., 105(D21), 26531–26546, 2000.
Pruppacher, H. R. and Klett, J. D.: Microphysics of Clouds and Precipitation, Kluwer Academic Publishers, Dordrecht, 1997.
Quinby-Hunt, M. S., Erskine, L. L., and Hunt, A. J.: Polarized light scattering by aerosols in the marine atmospheric boundary layer, Appl Opt., 36(21), 5168–5184, 1997.
Radke, L. F. and Hegg, D. A.: The shattering of saline droplets upon crystallization, J. Rech. Atmos., 6, 447–455, 1972.
Seinfeld, J. H.,and Pandis, S. N.: Atmospheric Chemistry and Physics – from Air Pollution to Climate Change, 2nd ed., John Wiley and Sons, Inc., New York, 1203 pp., 2006.
Shaw, G.: Production of condensation nuclei in clean air by nucleation of H_2SO_4, Atmos. Environ., 23, 2841–2846, 1989.
Tabata, S.: A simple but accurate formula for the saturation vapour pressure over liquid water,

ACPD
10, 26931–26959, 2010

J. Appl. Meteor., 12, 1410–1411, 1973.
Tolman, R. C.: The effect of droplet size on surface tension, J. Chem. Phys., 17, 333–337, 1949.
Twomey, S. and McMaster, K.: The production of condensation nuclei by crystallizing salt particles, Tellus, 7, 458–461, 1955.
Wehner, B., Siebert, H., Ansmann, A., Ditas, F., Seifert, P., Stratmann, F., Wiedensohler, A., Apituley, A., Shaw, R. A., Manninen, H. E., and Kulmala, M.: Observations of turbulence-induced new particle formation in the residual layer, Atmos. Chem. Phys., 10, 4319–4330, doi:10.5194/acp-10-4319-2010, 2010.
Whitby, K. T.: The physical characteristics of sulfur aerosols, Atmos. Environ., 12, 135–159, 1978.
Yu, F.: Effect of ammonia on new particle formation: a kinetic H_2SO_4-H_2O-NH_3 nucleation model constrained by laboratory measurements, J. Geophys. Res., 111, D01204, doi:10.1029/2005JD005968, 2006.
Yue, G. K. and Hamill, P.: The homogeneous nucleation rates of H_2SO_4-H_2O aerosol particles in air, J. Aerosol Sci., 10, 609–614, 1979.
Zhang, R., Suh, I., Zhao, J., Zhang, D., Fortner, E. C., Tie, X., Molina, L. T., and Molina, M. J.: Atmospheric new particle formation enhanced by organic acids, Science, 304, 1487–1490, 2004.

ACPD
10, 26931–26959, 2010

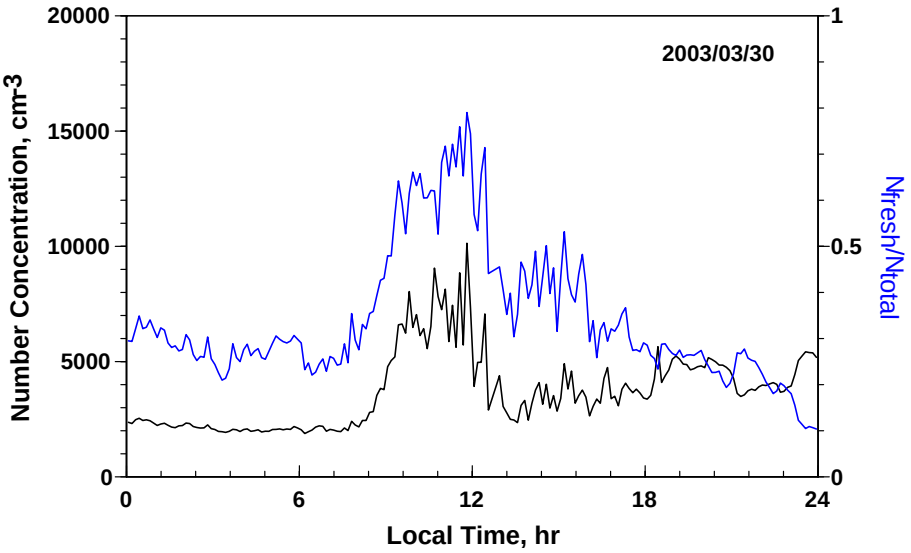

Fig. 1. Diurnal evolution of aerosol number concentration (filled dots, left axis) and fraction of fresh particle (solid line, right axis) for the 31 March 2003 case measured at a coastal site over Northern Taiwan. Fresh particles are defined as those with diameter smaller than 30 nm.

ACPD
10, 26931–26959, 2010

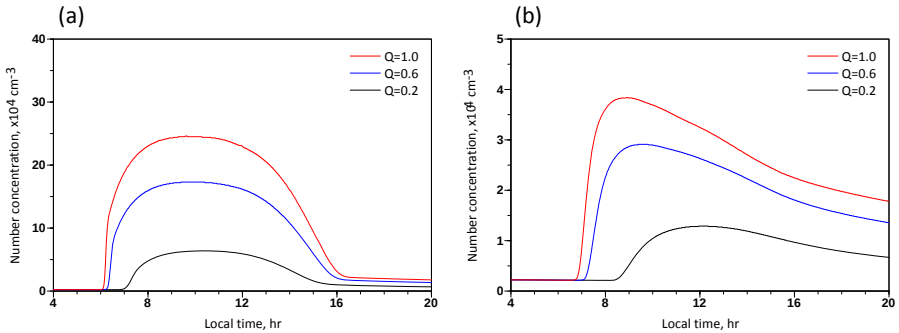

Fig. 2. Simulated diurnal evolution of aerosol number concentration for the conditions of Shimen with different actinic flux transmission ratios. **(a)** All particles (D-all); **(b)** particles with diameter greater than 10 nm (D>10).

ACPD
10, 26931–26959, 2010

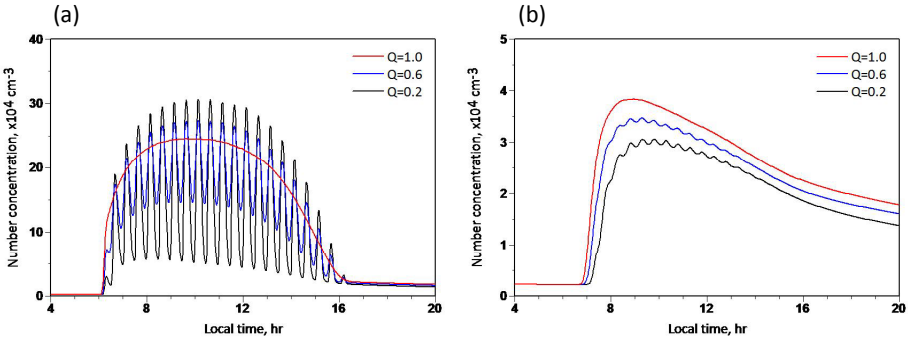

Fig. 3. Same as Fig. 2, but with the influence of stratocumulus cloud shadows. Various values of minimum transmission ratio *Q* were applied, but only a few selected ones are presented to avoid cluttering the figures.

ACPD
10, 26931–26959, 2010

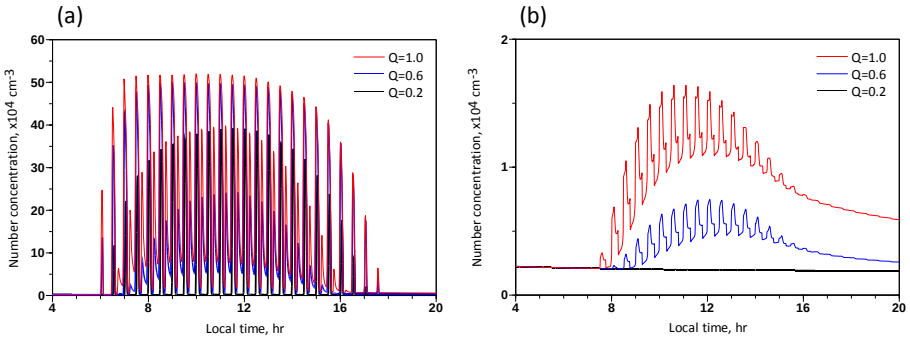

Fig. 4. Simulations of new particle production in air parcel moving in the form of large eddy circulation within the atmospheric boundary layer. The amplitude and period of the large eddy are set as 500 m and 30 min, respectively. The left panel shows the variation of D-all, and the right panel is for D>10.

ACPD
10, 26931–26959, 2010

Aerosol nucleation spikes in the planetary boundary layer

J.-P. Chen et al.

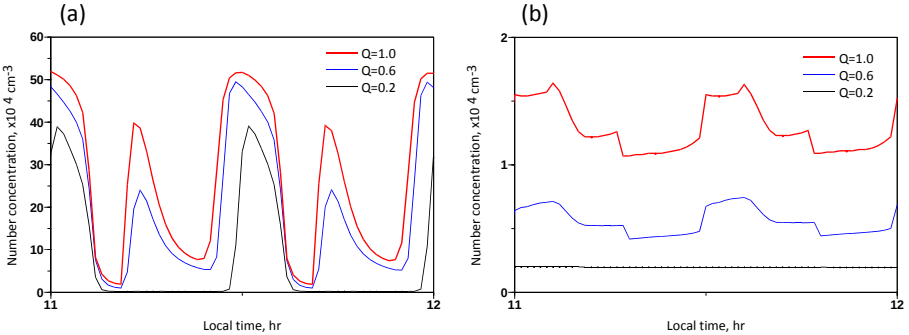

Fig. 5. Same as Fig. 4, but zoom up for the period between 11h00 and noon.

ACPD
10, 26931–26959, 2010

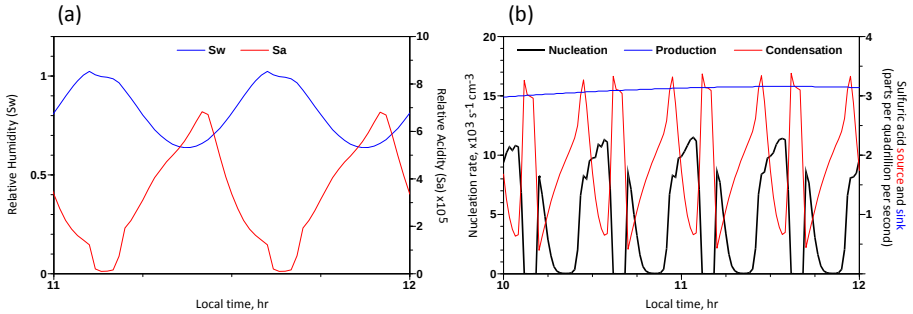

Fig. 6. Evolution of **(a)** relative humidity S_w and relative acidity S_a, and **(b)** rates of nucleation (per unit volume and unit time), as well as rates (in parts per quadrillion by volume per second) of photochemical production (dashed curve) and condensation (dotted curve) of sulfuric acid vapour for the case of Q=1 in Fig. 5. Time length shown is the same as in Fig. 5.

ACPD
10, 26931–26959, 2010

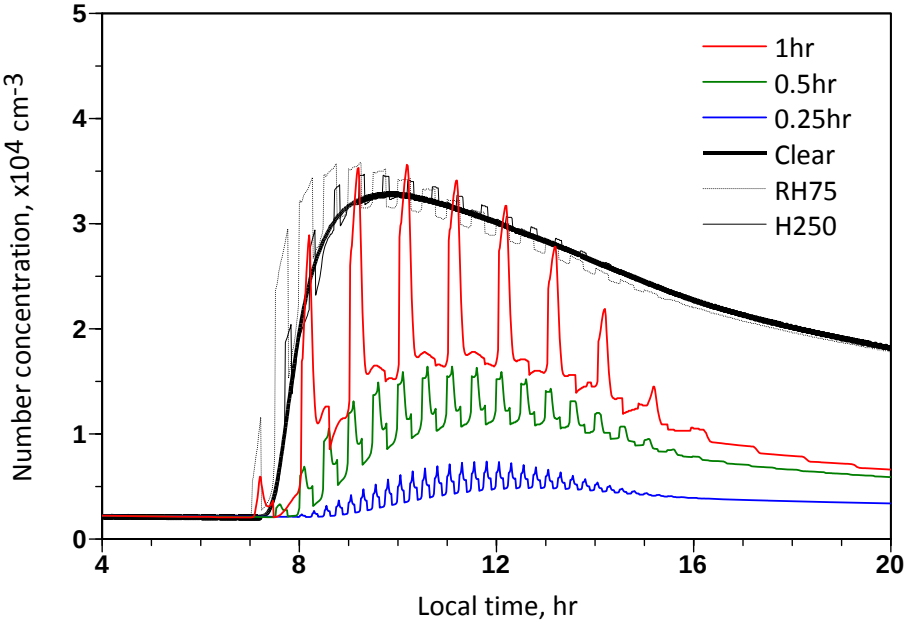

Fig. 7. Evolution of $D>10$ aerosol number concentrations under various scenarios of turbulence eddy. The green solid curve (cycle period 0.5 h) is the same as the $Q=1$ curve in Fig. 4b, and is called the reference run. The thick-solid curve is the same as the $Q=1$ curve in Fig. 3b, representing the clear sky situation without turbulence eddy. The red curve and the blue curve applied the same conditions as the reference run except for the cycling periods of 1 h and 0.25 h, respectively. The dash-dotted curve differs from the reference run in its lower (by 5%) initial relative humidity; while the thin solid curve applied a vertical amplitude that is one half of the reference run (a half-height of 250 m).

ACPD
10, 26931–26959, 2010